Author Manuscript

Author Manuscript

Author Manuscript

Author Manuscript

HHS Public Access

Author manuscript

J Tissue Eng Regen Med. Author manuscript; available in PMC 2019 June 01.

Published in final edited form as:

J Tissue Eng Regen Med. 2018 June ; 12(6): 1519–1529. doi:10.1002/term.2681.

Heparin-Dopamine Functionalized Graphene Foam for Sustained Release of Bone Morphogenetic Protein-2

Qingqing Yao[a,b,c,**], **Yangxi Liu**[c], and **Hongli Sun**[c,*]

[a]School of Ophthalmology and Optometry, Wenzhou Medical University, 270 Xueyuan Xi Road, Wenzhou, Zhejiang 325027, China

[b]Institute of Advanced Materials for Nano-Bio Applications, Wenzhou Medical University, Wenzhou, Zhejiang 325027, China

[c]Department of Biomedical Engineering, University of South Dakota, BioSNTR, Sioux Falls, SD 57107, USA

Abstract

The recently developed three-dimensional (3D) graphene foam (GrF) is intriguing for potential bone tissue engineering applications since it provides stem cells with a 3D porous substrate for osteogenic differentiation. However, the nature of graphene's structure lacks functional groups thus making it difficult for further modification such as immobilization or conjugation of growth factors, which are normally required to promote tissue regeneration. To explore the potential of GrF functionalization and sustained release of therapeutic proteins, we fabricated a modified 3D GrF scaffold with bio-inspired heparin-dopamine (Hepa-Dopa) molecules using a highly scalable chemical vapor deposition (CVD) method. Our data indicated Hepa-Dopa modification resulted in significantly higher bone morphogenetic protein-2 (BMP2) binding ability and longer release capacity compared to the untreated scaffolds. Importantly, the heparin-functionalized 3D GrF significantly improved the exogenous BMP2-induced osteogenic differentiation. Therefore, our study, for the first time, indicated that the 3D GrF can be bio-mimetically functionalized with Hepa-Dopa and be used for sustained release of BMP2, thereby inducing osteogenic differentiation and suggesting promising potential as a new multifunctional carrier for therapeutic proteins and stem cells in bone tissue engineering.

Keywords

Graphene foam; Bone morphogenetic protein-2 (BMP2); Heparin; Drug delivery; Osteogenic differentiation; Bone tissue engineering

1. Introduction

Repair of large bone defects remains a significant clinical challenge. While autologous bone graft is still considered the gold standard for most applications, it is limited by several

*Professor Hongli Sun, Ph.D., Phone: (+1) 605-275-7470; Fax: +1 605-782-3280; Hongli.Sun@usd.edu. **Professor Qingqing Yao, Ph.D., Phone: (+1) 605-251-5168; Fax: +1 605-394-1232; yaoqing400@163.com.

Author Manuscript Author Manuscript Author Manuscript Author Manuscript

factors. These factors include morbidity at the donor site and challenges associated with preparing anatomically-shaped grafts from harvested bone (Petite *et al.*, 2000 ; Schroeder *et al.*, 2011; Khan *et al.*, 2008; Grabowski *et al.*, 2013; Hong *et al.*, 2004). Bone tissue engineering is considered a promising alternative, with two of the most widely-studied tissue engineering approaches being biomaterials(scaffold)-mediated exogenous stem/progenitor cells transplantation (*e.g.*, bone marrow mesenchymal stem cells, BMSCs) and growth factors/hormones delivery (*e.g.*, bone morphogenetic protein, BMPs). FDA-approved BMP2 and BMP7, used successfully in the treatment of bone repair, recruits and induces endogenous stem/progenitor cells for osteogenic differentiation (Khosla *et al.*, 2008; Zheng *et al.*, 2010; Lu *et al.*, 2003). BMP-based therapy, however, has been significantly impeded in clinical practice due to several critical barriers: high dose, high costs, and serious side effects (Haidar *et al.*, 2009; Courvoisier *et al.*, 2014; Sheikh *et al.*, 2015; Gothard *et al.*, 2014; Siu *et al.*, 2011).

To address these challenges in the bone tissue engineering, one important strategy is to develop innovative, osteoinductive scaffolds because of their crucial roles in cell adhesion, proliferation, differentiation, and extracellular matrix (ECM) formation (Abedalwafa *et al.*, 2013; Dhandayuthapani *et al.*, 2011; Ou *et al.*, 2014), with the goal of promoting strong osteogenic differentiation and bone regeneration using low dosage of exogenous proteins.

Graphene and its derivatives are emerging as new types of material for biomedical applications because of their unique electrical, physical, and nanoscale properties, as well as excellent biocompatibility (Menaa *et al.*, 2015; Pattnaik *et al.*, 2016). Recently developed three-dimensional (3D) graphene foam (GrF) is particularly intriguing for potential bone tissue engineering application because, compared to a polymer scaffold, 3D GrF exhibits fascinating properties such as 1) high electrical conductivity (10 S cm^{-1}) to allow tissue stimulation (Li *et al.*, 2013); 2) ultralow density, which means less byproducts produced (for GrF ca. 5 mg cm^{-3}, for polymers ca. 88–138 g cm^{-3}) (Frydrych *et al.*, 2015; Loeblein *et al.*, 2016); 3) high porosity to enhance the oxygen diffusion (for GrF 99.7%, for polymers 91–95%) (Frydrych *et al.*, 2015), and 4) extremely high specific surface area for cell attachment (for GrF 850 m^2 g^{-1}, for polymers ca. 1–10 m^2 g^{-1}) (Menaa *et al.*, 2015; Krontiras *et al.*, 2015), which is advantageous for substrate-based drug delivery. Moreover, the tunable biodegradability of GrF via a two-step oxidative process that is preferable for tissue engineering application (Loeblein *et al.* 2016). Therefore, GrF is attractive for potential tissue engineering applications, where some initial studies indicated GrF supported stem cells for neural, osteogenic, and chondrogenic differentiation (Nieto *et al.*, 2015; Samad *et al.*, 2015; Wang *et al.*, 2015). Specifically, it was noted that 3D GrF was not only able to provide stem cells with a 3D substrate for attachment and growth, but also favorites osteogenic differentiation even without addition of osteogenic factors (*e.g.,* BMPs) (Crowder *et al.*, 2013).

However, the chemical structure of graphene lacks functional groups thus making it difficult for further modifications, including immobilization and/or conjugation of growth factors, which are normally required to promote tissue regeneration. For example, although GrF was shown to slightly promote osteogenic differentiation in the previous report (Crowder *et al.*, 2013), GrF alone was not enough to fully induce the stem cell osteogenic differentiation

Author Manuscript Author Manuscript Author Manuscript Author Manuscript

(from our preliminary data). Thus, extra osteogenic signals (*e.g.,* BMPs) are required to be persistently present in the scaffold. Moreover, considering the fast degradation and low efficacy of BMPs, a controlled release technique is highly desired. Heparin, a naturally sulfated biopolymer with a high negative charge in the ECM, can bind and stabilize positively charged heparin-binding proteins, including many growth factors (*e.g.,* BMPs) (Liang *et al.*, 2014; Azevedo *et al.*, 2015). These bio-inspired, affinity-based techniques have emerged as attractive strategies in developing heparin-modified materials for protein delivery (Vulic *et al.*, 2014). The absence of functional groups on the surface of graphene makes it difficult to be directly conjugated with heparin for BMPs release. Previously, a bio-inspired poly-dopamine coating strategy proved to be a versatile and simple route to functionalize bio-inert materials for biomedical applications (Lee *et al.*, 2007). Furthermore, the covalently jointed heparin-dopamine coating was reported initially as an effective method to functionalize titanium for sustained release of BMP2 by leveraging both functional moieties from the two molecules (Lee *et al.*, 2012).

Therefore, our hypothesis is that the 3D GrF can be bio-mimetically functionalized with heparin-dopamine and used for sustained release of BMP2, thereby inducing strong osteogenic differentiation with the perspective of being used as a new multifunctional carrier for therapeutic proteins and stem cells in bone tissue engineering.

2. Materials and Methods

2.1. Materials

Nickle foam was purchased from Taili (Suzhou, China). Poly (methyl methacrylate) (PMMA), (2-(Nmorpholino) ethanesulfonic acid) hydrate (MES), N-hydroxy-succinimide (NHS), heparin, bovine serum albumin, phosphate buffered saline, and cyclohexane were purchased from Sigma (St. Louis MO, USA). And 1-Ethyl-3-(3-dimethylaminopropyl) carbodiimide HCl (EDC) was purchased from Thermal Scientific (Rockford, USA).

2.2. Preparation of GrF and heparin modified GrF (GrF/Hepa) scaffolds

GrF was synthesized via a modified CVD method as described previously (Chen *et al.*, 2011). Briefly, nickel (Ni) foams (250–450 g/m^2, 2mm in thickness) were used as the 3D scaffold templates for the growth of graphene. The nickel foams were placed at the center of a quartz tubular furnace, which was heated at 1000 °C under N_2 (200 s.c.c.m.) and H_2 (60 s.c.c.m.) to remove the thin oxide layer on their surface. A small amount of CH_4 was then introduced into the reaction tube at ambient pressure. An ultra-thin layer of graphene film was deposited on the Ni template after 10 min. A thin layer of poly (methyl methacrylate) (PMMA) was introduced on the surface of the graphene films as a support to prevent the graphene network from collapsing during the removal of the nickel template. The Ni template was then removed by soaking into the diluted HNO_3/H_2O_2 solution at 80 °C. GrF were subsequently obtained after removing of PMMA in the hot acetone solution.

To immobilize BMP2 onto the surface of GrF, the surface of GrF was functionalized with Hepa-Dopa. In brief, heparin was conjugated with dopamine in an EDC/NHS system (Lee *et al.*, 2012). Heparin (400 mg), EDC (190.6 mg), and NHS (115 mg) were dissolved in 10 ml

Author Manuscript Author Manuscript Author Manuscript Author Manuscript

of MES buffer (pH 4.5) and allowed to react for 10 min at room temperature. Dopamine hydrochloride (102.2 mg) was then dissolved in 1 ml of MES buffer) and added to the prepared heparin solution and allowed to react overnight. The mixture was dialyzed (MWCO 2000; Thermal Scientific) against acidified distilled water for 3 days and lyophilized. To modify the GrF with heparin, Hep-Dopa compound was first dissolved in a Tris·HCl solution (pH 8.0) to a concentration of 10 mg/mL. GrF was then immersed in the prepared Hepa-Dopa solution and gently shaken for 24 h in the dark. The heparin-modified GrF was washed several times with DI water and lyophilized. The overall procedure was summarized in Figure 1.

2.3. Characterization of the GrF and GrF/Hepa scaffolds

The morphology of the GrF and GrF/Hepa scaffolds was determined by a scanning electron microscope (SEM, Zeiss Leica) at 10 kV accelerating voltage after the samples were coated with gold as previously described (Yao *et al.*, 2016). The surface chemistry of the scaffold was examined by a Multifunctional X-ray Photoelectron Spectroscope (XPS, AXIS ULTRA DLD) using an Al K. The C1s hydrocarbon peak at 284.6 eV was used as the reference for all binding energies. To determine the hydrophilic properties of GrF and surface modified GrF scaffolds, the contact angle of scaffolds was measured with a goniometer (VCA Optima, AST PRODUCTS INC) after these foams were pressed into 2D films with a flat surface.

2.4. *In vitro* BMP2 release

To prove the immobilization of BMP2 on the Hepa-Dopa modified GrF scaffold, we labelled the BMP2 protein with FITC (BMP2-FITC, Applied Biosystems) and observed by using confocal (FV1200, Olympus, Japan) microscopy imaging. Briefly, BMP2 solution was first mixed with FITC/PBS solution and shaking overnight at 4 °C. The mixed solution was then transferred into a dialysis tube (MWCO 3000, Thermal Scientific) and dialyzed for 3 days (fresh DI water was replaced every 8 h). The BMP2-FITC was then added onto GrF and GrF/Hepa scaffolds and incubated for 1 h at room temperature. The samples were then washed with PBS three times (10 min each time) to remove free BMP2-FITC before imaging by confocal. The effect of Hepa-Dopa modification on binding and release of human recombinant BMP2 (rhBMP2) on the scaffolds was analyzed through a human BMP2 ELISA Development kit (Peprotech, USA) as described previously (Yao *et al.*, 2016). Briefly, rhBMP2 was firstly dissolved in 0.1% BSA/PBS solution to make a stock solution with a final concentration of 100 μg/mL. 150 ng rhBMP2 (1.5μg/mL) was dropped on the prepared GrF, and GrF/Hepa scaffolds, respectively, and incubated for 1 h at room temperature. The samples were then washed with PBS three times (10 min each time) to remove free rhBMP2. After wash, rhBMP2 loaded samples were immersed in 1 mL PBS at 37 ºC and shaken at 100 rpm. Supernatant (0.5 mL) was collected and replaced with fresh PBS at 1, 3, 7, 24, 49, 72, 96, 120, 192, 246, 360, 408, 504 h after incubation. The amount of rhBMP2 was determined with the human BMP2 ELISA kit according to the manufacture's instruction.

Author Manuscript Author Manuscript Author Manuscript Author Manuscript

2.5. Assessment of bioactivity in simulated body fluid (SBF)

The mineralization process of GrF and GrF/Hepa scaffolds was studied in Kokubo's *simulated body fluid* (SBF) (Kokubo *et al.*, 1991) as we previously described (Yao *et al.*, 2017). Briefly, each sample was soaked in 10 mL of SBF and placed in an incubator at 37 °C with constant shaking at 60 rpm for 1 or 7 days. The SBF was refreshed twice a week. At the end of each incubation time, samples were removed from SBF, washed with de-ionized water, frozen at −20 °C overnight, and then freeze-dried for at least 24 h. The chemical compositions of scaffolds before and after SBF immersion were determined by attenuated total reflectance (ATR) spectroscopy (Nicolet, USA). The spectra were collected in transmission mode in the mid-IR range (4000–400 cm^{-1}).

2.6. Cell viability (MTS, CLSM)

The C2C12 cell was a generous gift from Dr. Yifan Li at the University of South Dakota. C2C12 (5×10^4 cells per well) were seeded onto GrF or GrF/Hepa scaffolds and cultured for 1 and 3 days. The cell viability of C2C12 on the scaffolds was studied by using MTS assay (Promega Corporation, USA) according to the manufacturers' instructions. GrF was selected as control and the cell viability was expressed as 100%.

Cells morphologies on scaffolds were visualized by staining with Texas red-X Phalloidin (Life technologies, OR, USA) and DAPI (Southern Biotech, Birmingham, AL), which label F-actin and cell nucleus, respectively (Yao *et al.*, 2016). Briefly, cell-seeded scaffolds were fixed in 3.7% paraformaldehyde for 10 min and permeabilized with 0.1% TritonX-100 for another 5 min. Thereafter, the samples were blocked with 1% bovine serum albumin for 30 min before they were stained with Texas red-X and DAPI for 20 and 5 min, respectively. The cells/scaffolds were imaged using a laser scanning microscope (FV1200, Olympus, Japan).

2.7. Alkalin Phosphatase (ALP) activity and calcium content

ALP activity was carried out using an EnzoLyte pNPP Alkaline Phosphatase Assay Kit (AnaSpec, San Jose, CA), as we previously described with some minor modifications (Yao *et al.*, 2016). Briefly, cells/scaffolds were rinsed with PBS solution and lysed with lysis buffer for 1–2 min at room temperature. The lysate was then transferred into a tube and centrifuged for 15 min at 2500 g at 4 °C. The collected supernatant or standard solution (50 μL) was mixed with *p*-nitrophenyl phosphate and incubated for 30 min at 37 °C. Following the incubation, the reaction was stopped by adding 100 μL terminated liquid. ALP activity was measured at 405 nm and normalized against total protein content. The total protein content was measured with a BCA kit (Thermo Scientific™, Waltham, MA) according to the manufacture's instruction. Briefly, 25 μL of the collected supernatant (the same from ALP activity) or standard solution was mixed with 200 μL BCA working reagent and incubated for 30 min at 37 °C. Following the incubation, the protein content was measured at 562 nm.

Human bone marrow mesenchymal stem cells were purchased from Lonza (Lonza Walkersville, Inc. US) to study cell mineralization on the scaffolds. The cell-scaffold constructs were examined for calcium deposition by using a total calcium LiquiColor® kit (Stanbio laboratory, TX) as we described previously [34]. Briefly, after 3 weeks of culture, cells/scaffolds were rinsed with DPBS and cut into small pieces with a sharp blade. The

Author Manuscript Author Manuscript Author Manuscript Author Manuscript

calcium was extracted by using 1 mL 6 M hydrochloric acid. Thereafter, 10 μL extraction solution or 10 μL standard solution was added into 1 mL working solution prepared according to the manufacturer's instruction. The absorbance was measured at 550 nm, and the calcium content was calculated.

2.8. Gene expression analysis

Quantitative gene expression analysis was carried out as we previously described (Yao *et al.*, 2016) with some minor modifications. Briefly, total RNA was extracted using the GeneJET™ RNA Purification Kit (Thermo Scientific™, Waltham, MA) by following the manufacturer's instruction. RNA concentration was measured by UV–Vis spectroscopy (DU 730, Beckman coulter) at 260 nm and an equivalent amount of RNA was processed to generate cDNA by using the High Capacity cDNA Reverse Transcript kit purchased from Applied Biosystems (Forster City, CA). Quantitative PCR was performed with Taqman gene expression assays (Applied Biosystems, Forster City, CA) using the Applied Biosystems 7500 Fast Real-Time PCR System (Applied Biosystems, Carlsbad, CA). Triplicates were performed for each sample, and results were normalized to GAPDH. TaqMan® Gene Expression Assays of GAPDH (Mm99999915), RUNX2 (MmCG122221), BSP (Mm00436767), and OCN (Mm03413826) were purchased from Applied Biosystems (Forster City, CA).

2.9. Statistical analysis and image editing

To determine statistical significance of observed differences between the study groups, a two-tailed homoscedastic t-test was applied. A value of $p < 0.05$ was considered to be statistically significant. Values are reported as the mean ± one standard deviation (SD). Brightness and contrast were adjusted equally across all the images for improved visibility.

3. Results

3.1. Morphologies and properties of the scaffolds

The 3D GrF was synthesized by CVD method on a Ni foam template. The surface morphologies of GrF and GrF/Hepa scaffolds were studied by SEM (Figure 2). GrF showed a continuous interconnected porous structure with a porosity around 95% and contained a pore size of 278.2±69.5 μm and a 52.3±9.2 μm thick foam walls. The GrF surface was covered with many ripples and wrinkles, which may be due to different thermal expansion coefficients between Ni and graphene during the CVD process (Li *et al.*, 2013; Crowder *et al.*, 2013). The elemental chemical compositions of GrF, GrF/Hepa and GrF/Hepa/BMP2 scaffolds were shown in Figure 3 and Table 1 based on XPS analysis. There were significant increases in the contents of O, N, and S element on the GrF/Hepa samples compared to neat GrF samples that suggested Hepa-Dopa molecules were successfully immobilized onto the GrF scaffold surfaces. As the 1H NMR spectra (Figure S1) shown, the peaks between 6.5~7.5 ppm (a, b) on Hepa-Dopa (B) were attributed to the aromatic protons on the dopamine. The peaks on Hepa-Dopa around 2.6 and 2.8 ppm (c,d) were the ethyl groups from dopamine. All peaks (a–d) from Hepa-Dopa (B) were not identified on Hep (A), which confirmed the successful synthesis of Hepa-Dopa. Moreover, after incubation with rhBMP2 and extensive washes, the GrF/Hepa scaffolds showed a significant increase in N content

Author Manuscript Author Manuscript Author Manuscript Author Manuscript

(from 3.08% to 9.01%), and a decrease of C content (from 72.22% to 67.24%), suggesting that a large amount of rhBMP2 was captured by the heparin-functionalized GrF scaffolds. To investigate the hydrophilic property changes after the surface modifications, contact angle of the scaffolds was examined and the data were shown in Table 2. The water contact angle of GrF (107.4°±3.8°) was significantly decreased by the Hepa-Dopa modification (67.2°±5.9°). Moreover, the hydrophilicity of the Hepa-Dopa-modified scaffolds was further improved by rhBMP2 binding (from 67.2°±5.9° to 32.5°±3.9°).

To study the *in vitro* bioactivity of GrF and GrF/Hepa scaffolds, the prepared scaffolds were immersed in SBF for 1 or 7 days. No obvious apatite-like deposits were observed on GrF scaffolds after immersion in SBF for 1 and 7 days using SEM (Figure 4A, C). Compared to GrF samples, a few hydroxyapatite (HA)-like granular were developed on the GrF/Hepa scaffolds after 1 day of immersion in SBF (Figure 4B), while a higher amount of apatite were observed after 7 days (Figure 4D). These data indicated that the surface modification with Hepa-Dopa significantly improved the bioactivity. *In vitro* HA formation of GrF scaffolds was further supported by the ATR data (Figure S2). After 1 day of immersion in SBF, the characteristic peaks around 631 cm^{-1}, which is attributed to the OH^- groups, and the characteristic peaks at 1034 cm^{-1} and 1627 cm^{-1}, which are attributed to P-O bond in HA, were detected on the GrF/Hepa scaffolds. No such characteristic peaks were observed on the GrF scaffolds even after 7 days of immersion in SBF.

3.2. *In vitro* bioactivity of 3D scaffolds

3.2. BMP2 release from Heparin-decorated scaffolds

To study the BMP2 binding ability of the heparin-immobilized scaffolds, we firstly demonstrated the heparin-modified scaffolds (GrF/Hepa) had more BMP2-FITC binding compared to the control group (GrF) (Figure S4). Furthermore, the rhBMP2 release profiles from GrF and GrF/Hepa were studied by using ELISA assay (Figure 5). At the beginning, equal amount of BMP2 (*i.e.*, 150 ng per scaffold) was added to the GrF (neat scaffold as control) or GrF/Hepa (modified scaffold with heparin). Our ELISA data indicated that there were around 69.4 and 106 ng remained on each GrF and GrF/Hepa scaffold, respectively. Therefore, the heparin modified scaffolds (GrF/Hepa) had significantly higher BMP2 binding capacity compared to the control group (GrF scaffolds). It was observed that the rhBMP2 loaded on the GrF scaffolds was completely released in the first 72 h. On the contrary, rhBMP2 loaded on the heparin-immobilized GrF scaffold exhibited sustained release over the whole 21-day period. The total amounts of rhBMP2 released from the heparin-modified GrF scaffolds were significantly higher than the amounts released from the neat GrF scaffolds (51.2 ng *vs* 33.3 ng) during the 21-day release period, even though the same amounts of rhBMP2 were loaded onto each scaffold (150 ng per scaffold) at the beginning.

3.3. Cell viability and morphology on 3D scaffolds

The cell viabilities of C2C12 on GrF and GrF/Hepa scaffolds were quantitatively measured by MTS assay after culturing for 1 and 3 days. As shown in Figure 6A, both scaffolds exhibited similar cell viabilities after 1 day of culture. However, slightly higher cell viability on the GrF/Hepa scaffolds was observed after 3 days of cell culture ($p < 0.05$). This result

Author Manuscript Author Manuscript Author Manuscript Author Manuscript

demonstrated that the presence of Hepa-Dopa on the scaffolds was favorable for cell viability and proliferation, where more cells were observed using confocal microscopy on GrF/Hepa scaffolds (Figure 6B2&B4) compared to GrF scaffolds (Figure 6B1&B3) and no obvious differences in cell morphology were observed between the two types of scaffolds. These results suggested that the surface modification of GrF with Hepa-Dopa slightly increased cell viability with little impact on the cell morphology of C2C12.

3.4. Osteogenic differentiation of cells on 3D scaffolds

To study the effects of Hepa-Dopa modification on rhBMP2-induced osteogenic differentiation, C2C12 cells were seeded on GrF and GrF/Hepa scaffolds, which were both supplemented with same amount of rhBMP2 (200 ng/per scaffold) before cell seeding. The early osteogenic differentiation marker, ALP activity, was measured after 7 and 14 days of culture. As the data shown (Figure 7A, B), the cells cultured on GrF/Hepa/BMP2 scaffolds exhibited significantly higher ALP activity compared to that on GrF/BMP2 scaffolds for 7 and 14 days, respectively ($p < 0.01$ and $p < 0.05$). Moreover, the mineralization, formed at the late stage of osteogenic differentiation, was studied through analyzing the total calcium content produced by hMSCs after three weeks of culture. Although very little calcium was detected on either GrF or GrF/Hepa scaffold, extensive amount of calcium was produced by both GrF/BMP2 and GrF/Hepa/BMP2 scaffolds after three weeks (Figure 7C). It was noted that significantly higher amount of calcium was produced from GrF/Hepa/BMP2 scaffolds compared to that from GrF/BMP2 scaffolds ($p < 0.05$). Consistent with the ALP activity and calcium content data, the quantitative gene expression results (Figure 7D–F) also indicated that C2C12 on GrF/Hepa/BMP2 scaffolds had significantly higher levels of osteogenic gene expressions, including RUNX2, BSP and OCN, than the C2C12 cells cultured on GrF/BMP2 scaffolds. These results indicated that the immobilization of Hepa-Dopa onto GrF scaffolds significantly improved rhBMP2-induced osteogenic differentiation.

Interestingly, it was noted that Hepa-Dopa modification consistently decreased the expression levels of all the osteogenic genes (*i.e.,* RUNX2, BSP, and OCN) on the scaffolds in the absence of exogenous rhBMP2 (Figure 7D–F). In order to study the potential mechanisms of the decreased osteogenic capacity of the modified scaffolds, we tested the effects of heparin on osteogenic differentiation in the conditions of presence or absence of exogenous rhBMP2. As our data indicated, in both conditions, with (Figure S5B) or without (Figure S5A) 100 ng/mL of exogenous rhBMP2 presence in the culture medium, heparin at low dose (0.5 μg/mL) significantly decreased ALP activity, while increasing ALP activity at high dose (50 μg/mL). Therefore, heparin could significantly affect the ALP activity of C2C12 cells in a highly dose-dependent manner. Furthermore, we studied if the dopamine or Hepa-Dopa modifications could influence osteogenic differentiation. Based on the gene expression data, we found both late stage osteogenic markers, BSP and OCN expression levels, were reduced by either dopamine or Hepa-Dopa coating, while no significant changes were observed for the early osteogenic marker RUNX2 expression (Figure S6). Overall, the presences of heparin and dopamine/Dop-Hepa on the GrF scaffolds could influence osteogenic differentiation.

Author Manuscript Author Manuscript Author Manuscript Author Manuscript

4. Discussion

Graphene and its derivatives have a high drug loading capacity largely because of the enormous surface area as well as the planar aromatic structure, which offer an excellent capability to immobilize many substances through π-π stacking, hydrophobic interaction, and hydrogen bonding (Sanchez *et al.*, 2012). In addition to drug delivery, graphene and graphene oxide sheets improved stem cells osteogenic differentiation when coated or mixed with other materials, but the mechanisms remain elusive (Shadjou *et al.*, 2016; Lee *et al.*, 2011). In contrast to most graphene/graphene oxides sheets-based composite materials, the 3D GrF was developed by a new template-directed CVD technique with improved electrical conductivity in addition to the highly porous macro-structure (Chen *et al.*, 2011), which are advantageous for tissue engineering applications. Notably, one recent study reported that the 3D GrF was able to promote hMSCs to spontaneously differentiate into osteoblasts without the addition of osteogenic medium or mediators (Crowder *et al.*, 2013), while the graphene or graphene oxide modified materials could only improve osteogenic differentiation of hMSCs in the presence of osteogenic medium by pre-concentrating with osteogenic factors (Lee *et al.*, 2011). This suggested GrF provides a favorable 3D microenvironment for stem cell osteogenic differentiation, thus we developed the 3D GrFs using the same technique to study if they can support sustained release of BMP2 since it is critical for the success of bone tissue engineering. Consistent with previous reports (Crowder *et al.*, 2013; Chen *et al.*, 2011), our 3D GrFs demonstrated interconnected macro-pore structures with very high porosity (95%). Our data indicated that the absorbed rhBMP2 was completely released from the neat 3D GrFs in less than three days (Figure 5 black line), which was different from the longer sustained release of BMP2 observed on the 2D graphene oxide nanosheets/flakes (La *et al.*, 2011; Zhong *et al.*, 2011). Although the mechanism of BMP2 release from graphene materials is still elusive, this finding urges the need to develop a new strategy to improve BMP2 release capability of 3D GrFs.

Inspired by the high affinity of heparin to BMPs, we immobilized heparin onto the 3D GrF by using dopamine as a linker because the ortho-dihydroxyphenyl functional group in dopamine can form strong covalent and noncovalent bonds with a variety of materials (Kim *et al.*, 2014; Kim *et al.*, 2011; Bhakta *et al.*, 2011). The surface modification with Hepa-Dopa molecules did not significantly affect the macrostructure of the scaffolds, but greatly increased the hydrophilicity of the materials' surface based on our data. Consequently, the GrF/Hepa showed significantly improved HA formation ability in SBF, which is one of desired features of biomaterials used in bone tissue engineering (Liang *et al.*, 2014). Additionally, higher cell viability on the modified scaffolds was observed compared to the neat scaffolds. These data indicated that the bioactivity of graphene was improved after surface modification, which may be attributed to the improved hydrophilicity and subtle surface morphology changes of graphene. Most importantly, the functionalized GrFs can provide sustained BMP2 release for over 21 days, while the neat GrF lasted less than three days. Consistently, the low dose of rhBMP2 (200 ng/per scaffold) that was applied only once induced significantly stronger osteogenic differentiation in both C2C12 and hMSCs on the heparin-functionalized groups than the control neat scaffolds.

Author Manuscript Author Manuscript Author Manuscript Author Manuscript

However, it was not expected that the Hepa-Dopa, when cultured in growth medium without the addition of exogenous rhBMP2, consistently reduced the basic expression levels of all three osteoblastic marker genes in C2C12. It is generally believed that heparin can bind with BMP2, thereby stabilizing and further improving the efficacy of BMP2 *in vitro*. Yet the role of heparin in sustaining the biological activity of BMP2 seems complicated and has not been fully elucidated. For example, it was reported that heparin can inhibit the BMP2-induced osteogenic activity by binding to both BMP2 and BMP receptor (BMPR) (Kanzaki *et al.*, 2008). Moreover, heparin either reduced or increased BMP2-induced osteogenic differentiation in MC3T3-E1 cell for different culture durations (Kanzaki *et al.*, 2011). Our studies indicated that heparin significantly affected C2C12 osteogenic differentiation in a dose-dependent manner in both the presence and absence of exogenous rhBMP2 in the medium (Figure S5). Furthermore, we also investigated the potential effects of the dopamine and Hepa-Dopa modifications on osteogenic differentiation on the GrFs. Interestingly, we found both modifications reduced the osteogenic markers although to different extents (Figure S6), which revealed some features of 3D GrF (*e.g.* charge, hydrophobicity) may be important for improving osteogenic marker expressions as previously reported (Crowder *et al.*, 2013; Lee *et al.*, 2011). Although more studies will be needed to understand the underlying mechanisms, it should be noted that either heparin or Hepa-Dopa only slightly affected the basal level of osteogenic markers, which were negligible compared to the Hepa-Dopa-captured exogenous rhBMP2 that induced overall osteogenic differentiation (Figure 6). As a new scaffold, there are still a lot of potential issues with GrFs to be addressed before moving onto the next step, *e.g.,* mechanical properties, safety, and degradation *in vivo*. Nevertheless, our studies proved the feasibility, for the first time, that 3D GrFs can be functionalized and used for sustained release of BMP2 to induce potent stem cell osteogenic differentiation and mineralization on the scaffolds.

5. Conclusion

In the present work, the 3D graphene foams with strong rhBMP2 binding affinity were successfully prepared by immobilizing heparin onto the scaffolds via a biomimetic dopamine linker. Our data indicated that Hepa-Dopa modification increased the *in vitro* bioactivity and cell viability on the scaffolds without compromising the macro-porous structure of the 3D GrF scaffolds. Importantly, heparin-decorated GrF showed significantly higher BMP2 binding ability and longer release capability compared to the untreated scaffolds. Consequently, the heparin-functionalized GrF significantly improved the exogenous BMP2-induced osteogenic differentiation on the 3D scaffolds. Therefore, our study, for the first time, indicated that the 3D GrF can be bio-mimetically functionalized with Hepa-Dopa and used for sustained release of BMP2, thus inducing osteogenic differentiation and signifying a potentially new multifunctional carrier for therapeutic proteins and stem cells in bone tissue engineering.

Acknowledgments

Financial support for this work from the Chinese National Nature Science Foundation (31600773) and the Zhejiang National Nature Science Foundations (LQ16H180003) is acknowledged. This work was also supported by NIH/NIDCRR03 DE027491 (H.S.) and the National Science Foundation/EPSCoR (Award IIA-1335423).

Author Manuscript Author Manuscript Author Manuscript Author Manuscript

References

Abedalwafa M, Wang F, Wang L, et al. Biodegradable poly-epsilon-caprolactone (PCL) for tissue engineering applications: a review. Rev Adv Mater Sci. 2013; 34:123–140.

Bhakta G, Rai B, Lim ZX, et al. Hyaluronic acid-based hydrogels functionalized with heparin that support controlled release of bioactive BMP-2. Biomaterials. 2012; 33:6113–6122. [PubMed: 22687758]

Bouxsein M, Turek T, Blake C, et al. Recombinant human bone morphogenetic protein-2 accelerates healing in a rabbit ulnar osteotomy model. J Bone Joint Surg Am. 2001; 83:1219–1230. [PubMed: 11507131]

Carreira A, Lojudice F, Halcsik E, et al. Bone morphogenetic proteins facts, challenges, and future perspectives. J Dent Res. 2014; 93:335–345. [PubMed: 24389809]

Chen Z, Ren W, Gao L, et al. Three-dimensional flexible and conductive interconnected graphene networks grown by chemical vapour deposition. Nat Mater. 2011; 10:424–428. [PubMed: 21478883]

Courvoisier A, Sailhan F, Laffenetre O, et al. Bone morphogenetic protein and orthopaedic surgery: Can we legitimate its off-label use? Int Orthop. 2014; 38:2601–2605. [PubMed: 25267430]

Crowder SW, Prasai D, Rath R, et al. Three-dimensional graphene foams promote osteogenic differentiation of human mesenchymal stem cells. Nanoscale. 2013; 5:4171–4176. [PubMed: 23592029]

Dhandayuthapani B, Yoshida Y, Maekawa T, et al. Polymeric scaffolds in tissue engineering application: a review. Inter J Polymer Sci. 2011:290602.

Frydrych M, Román S, MacNeil S, et al. Biomimetic poly (glycerol sebacate)/poly (l-lactic acid) blend scaffolds for adipose tissue engineering. Acta Biomater. 2015; 18:40–49. [PubMed: 25769230]

Geiger M, Li R, Friess W. Collagen sponges for bone regeneration with rhBMP2. J Clin Periodontol. 2003; 55:1613–1629.

Gothard D, Smith EL, Kanczler JM, et al. Tissue Engineered Bone Using Select Growth Factors: A Comprehensive Review of Animal Studies and Clinical Translation Studies in Man. Eur Cells Mater. 2014; 28:166–208.

Grabowski G, Cornett CA. Bone Graft and Bone Graft Substitutes in Spine Surgery: Current Concepts and Controversies. J Am Acad Orthop Surg. 21:51–60.

Haidar ZS, Hamdy RC, Tabrizian M. Delivery of recombinant bone morphogenetic proteins for bone regeneration and repair. Part A: Current challenges in BMP delivery. Biotechnol Lett. 2009; 31:1817–1824. [PubMed: 19690804]

Hong J, Cabe GD, Tedrow JR, et al. Failure of trabecular bone with simulated lytic defects can be predicted non-invasively by structural analysis. J Orthop Res. 2004; 22:479–486. [PubMed: 15099624]

Kanzaki S, Ariyoshi W, Takahashi T, et al. Dual effects of heparin on BMP-2-induced osteogenic activity in MC3T3-E1 cells. Pharmacol Rep. 2011; 63:1222–1230. [PubMed: 22180365]

Kanzaki S, Takahashi T, Kanno T, et al. Heparin inhibits BMP-2 osteogenic bioactivity by binding to both BMP-2 and BMP receptor. J Cell Physiol. 2008; 216:844–850. [PubMed: 18449905]

Khan Y, Yaszemski MJ, Mikos AG, et al. Tissue Engineering of Bone: Material and Matrix Considerations. J Bone Joint Surg Am. 2008; 1:36–42.

Khosla S, Westendorf JJ, Oursler MJ. Building bone to reverse osteoporosis and repair fractures. J Clin Invest. 2008; 118:421–428. [PubMed: 18246192]

Kim SE, Song S-H, Yun YP, et al. The effect of immobilization of heparin and bone morphogenic protein-2 (BMP-2) to titanium surfaces on inflammation and osteoblast function. Biomaterials. 2011; 32:366–373. [PubMed: 20880582]

Kiew SF, Liew LV, Lee HB, et al. Assessing biocompatibility of graphene oxide-based nanocarriers: A review. J Control Release. 2016; 226:217–228. [PubMed: 26873333]

Kokubo T. Bioactive glass ceramics: properties and applications. Biomaterials. 1991; 12:155–163. [PubMed: 1878450]

Author Manuscript Author Manuscript Author Manuscript Author Manuscript

Krontiras P, Gatenholm P, Hägg DA. Adipogenic differentiation of stem cells in three-dimensional porous bacterial nanocellulose scaffolds. J Biomed Mater Res B Appl Biomater. 2015; 103:195–203. [PubMed: 24819827]

La WG, Park S, Yonn HH, et al. Delivery of a therapeutic protein for bone regeneration from a substrate coated with graphene oxide. Small. 2013; 9:4051–4060. [PubMed: 23839958]

Lee DW, Yun YP, Park K, et al. Gentamicin and bone morphogenic protein-2 (BMP-2)-delivering heparinized-titanium implant with enhanced antibacterial activity and osteointegration. Bone. 2012; 50:974–982. [PubMed: 22289658]

Lee H, Dellatore SM, Miller WM, et al. Mussel-inspired surface chemistry for multifunctional coatings. Science. 2007; 318:426–430. [PubMed: 17947576]

Lee WC, Lim CHYX, Shi H, et al. Origin of Enhanced Stem Cell Growth and Differentiation on Graphene and Graphene Oxide. ACS Nano. 2011; 5:7334–7341. [PubMed: 21793541]

Liang Y, Kiick KL. Heparin-functionalized polymeric biomaterials in tissue engineering and drug delivery applications. Acta Biomater. 2014; 10:1588–1600. [PubMed: 23911941]

Li N, Zhang Q, Gao S, et al. Three-dimensional graphene foam as a biocompatible and conductive scaffold for neural stem cells. Sci Rep. 2013:3.

Liu J, Cui L, Losic D. Graphene and graphene oxide as new nanocarriers for drug delivery applications. Acta Biomater. 2013; 9:9243–9257. [PubMed: 23958782]

Loeblein M, Perry G, Tsang SH, et al. Three-Dimensional Graphene: A Biocompatible and Biodegradable Scaffold with Enhanced Oxygenation. Adv Healthc Mater. 2016; 5:1177–1191. [PubMed: 26946189]

Lu HH, Kofron MD, El-Amin SF, et al. In vitro bone formation using muscle-derived cells: a new paradigm for bone tissue engineering using polymer–bone morphogenetic protein matrices. Biochem Biophys Res Commun. 2003; 305:882–889. [PubMed: 12767913]

Menaa F, Abdelghani A, Menaa B. Graphene nanomaterials as biocompatible and conductive scaffolds for stem cells: impact for tissue engineering and regenerative medicine. J Tissue Eng Regen Med. 2015; 9:1321–1338. [PubMed: 24917559]

Mont MA, Ragland PS, Biggins B, et al. Use of bone morphogenetic proteins for musculoskeletal applications. J Bone Joint Surg Am. 2004; 86:41–55. [PubMed: 15691108]

Nieto A, Dua R, Zhang C, et al. Three Dimensional Graphene Foam/Polymer Hybrid as a High Strength Biocompatible Scaffold. Adv Funct Mater. 2015; 25:3916–3924.

Ou K-L, Hosseinkhani H. Development of 3D in vitro technology for medical applications. Inter J Mol Sci. 2014; 15:17938–17962.

Pattnaik S, Swain K, Lin ZQ. Graphene and graphene-based nanocomposites: biomedical applications and biosafety. J Mater Chem B. 2016; 4:7813–7831.

Petite H, Viateau V, Bensaïd W, et al. Tissue-engineered bone regeneration. Nat Biotechnol. 2000; 18:959. [PubMed: 10973216]

Sanchez VC, Jachak A, Hurt RH, et al. Biological interactions of graphene-family nanomaterials: an interdisciplinary review. Chem Res Toxicol. 2012; 25:15–34. [PubMed: 21954945]

Samad YA, Li Y, Alhassan SM, et al. Novel graphene foam composite with adjustable sensitivity for sensor applications. ACS Appl Mater Interfaces. 2015; 7:9195–9202. [PubMed: 25872792]

Schroeder JE, Mosheiff R. Tissue engineering approaches for bone repair: Concepts and evidence. Injury. 2011; 42:609–613. [PubMed: 21489529]

Seeherman H, Wozney JM. Delivery of bone morphogenetic proteins for orthopedic tissue regeneration. Cytokine Growth Factor Rev. 2005; 16:329–345. [PubMed: 15936978]

Shadjou N, Hasanzadeh M. Graphene and its nanostructure derivatives for use in bone tissue engineering: Recent advances. J Biomed Mater Res Part A. 2016; 104:1250–1275.

Sheikh Z, Javaid MA, Hamdan N, et al. Bone Regeneration Using Bone Morphogenetic Proteins and Various Biomaterial Carriers. Materials. 2015; 8:1778–1816. [PubMed: 28788032]

Siu RK, Lu SS, Li W, et al. Nell-1 Protein Promotes Bone Formation in a Sheep Spinal Fusion Model. Tissue Eng Part A. 2011; 17:1123–1135. [PubMed: 21128865]

Vulic K, Shoichet MS. Affinity–based drug delivery systems for tissue repair and regeneration. Biomacromolecules. 2014; 15:3867–3880. [PubMed: 25230248]

Author Manuscript Author Manuscript Author Manuscript Author Manuscript

Wang JK, Xiong GM, Zhu M, et al. Polymer-enriched 3D graphene foams for biomedical applications. ACS Appl Mater Interfaces. 2015; 7:8275–8283. [PubMed: 25822669]

Yao Q, Cosme JG, Xu T, et al. Three dimensional electrospun PCL/PLA blend nanofibrous scaffolds with significantly improved stem cells osteogenic differentiation and cranial bone formation. Biomaterials. 2017; 115:115–127. [PubMed: 27886552]

Yao Q, Liu Y, Tao J, et al. Hypoxia-mimicking nanofibrous scaffolds promote endogenous bone regeneration. ACS Appl Mater Interfaces. 2016; 8:32450–32459. [PubMed: 27809470]

Zheng Z, Yin W, Zara JN, et al. The use of BMP-2 coupled-Nanosilver-PLGA composite grafts to induce bone repair in grossly infected segmental defects. Biomaterials. 2010; 31:9293–9300. [PubMed: 20864167]

Zhong C, Feng J, Lin X, et al. Continuous release of bone morphogenetic protein-2 through nano-graphene oxide-based delivery influences the activation of the NF-κB signal transduction pathway. Int J Nanomedicine. 2017; 13:1215–1226.

Author Manuscript Author Manuscript Author Manuscript Author Manuscript

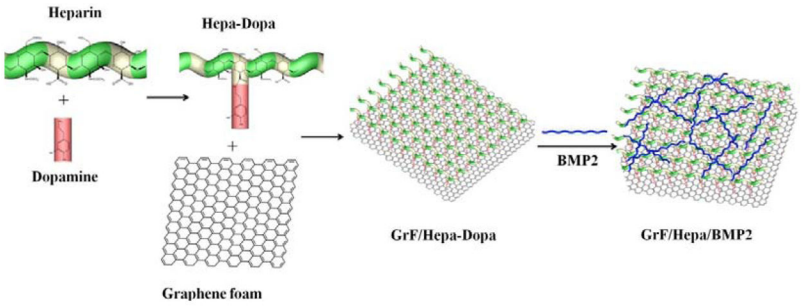

Figure 1.
Schematic procedure to prepare GrF/Hepa/BMP2 scaffolds.

Author Manuscript Author Manuscript Author Manuscript Author Manuscript

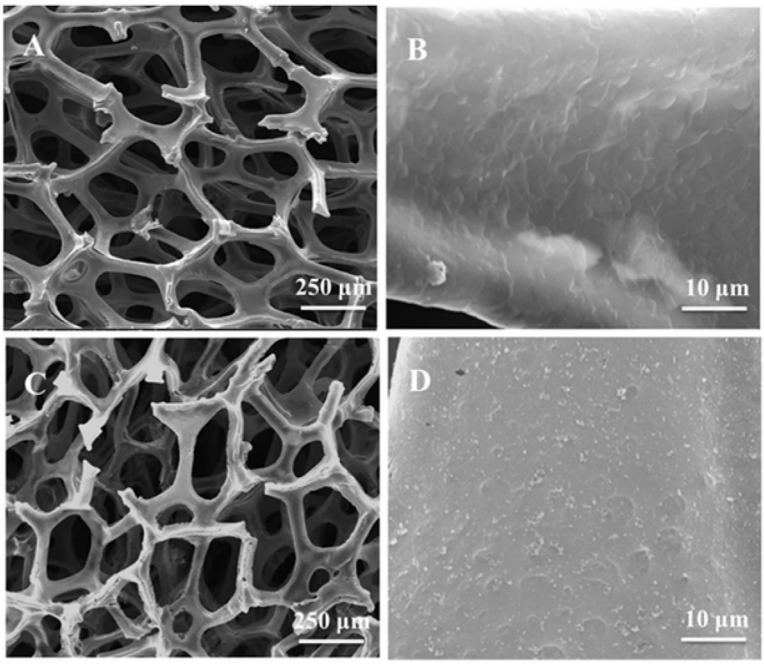

Figure 2.
SEM images of (A, B) GrF and (C, D) GrF/Hepa scaffolds.

Author Manuscript Author Manuscript Author Manuscript Author Manuscript

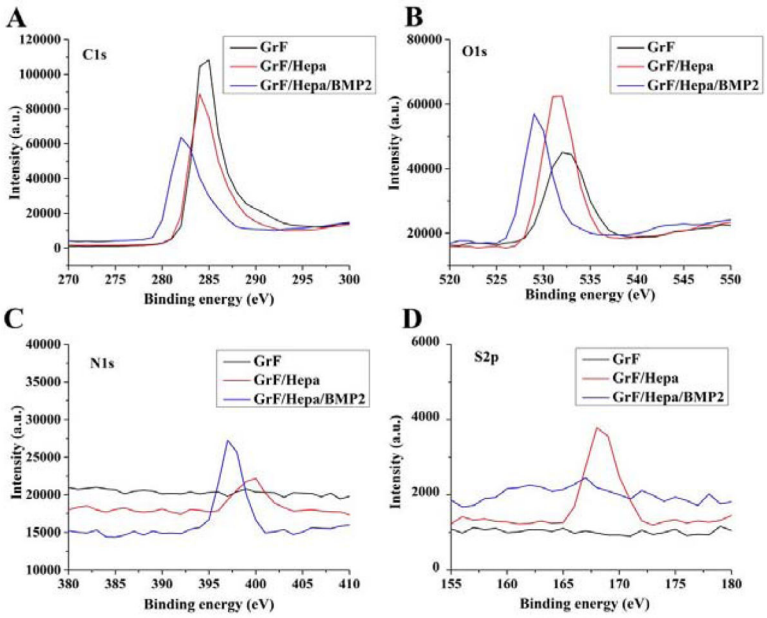

Figure 3.

Representative XPS wide-spectra of GrF, GrF/Hepa and GrF/Hepa/BMP2: (A) C1s, (B) O1s, (C) N1s and (D) S2p spectra.

Author Manuscript Author Manuscript Author Manuscript Author Manuscript

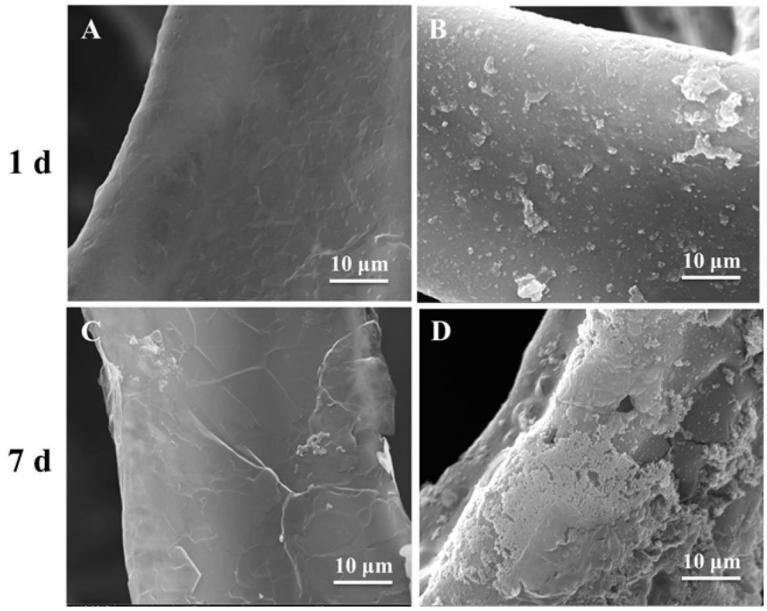

Figure 4.
SEM images of GrF and GrF/Hepa immersed in SBF after 1 and 7 days: (A, C) GrF, (B, D) GrF/Hepa.

Author Manuscript Author Manuscript Author Manuscript Author Manuscript

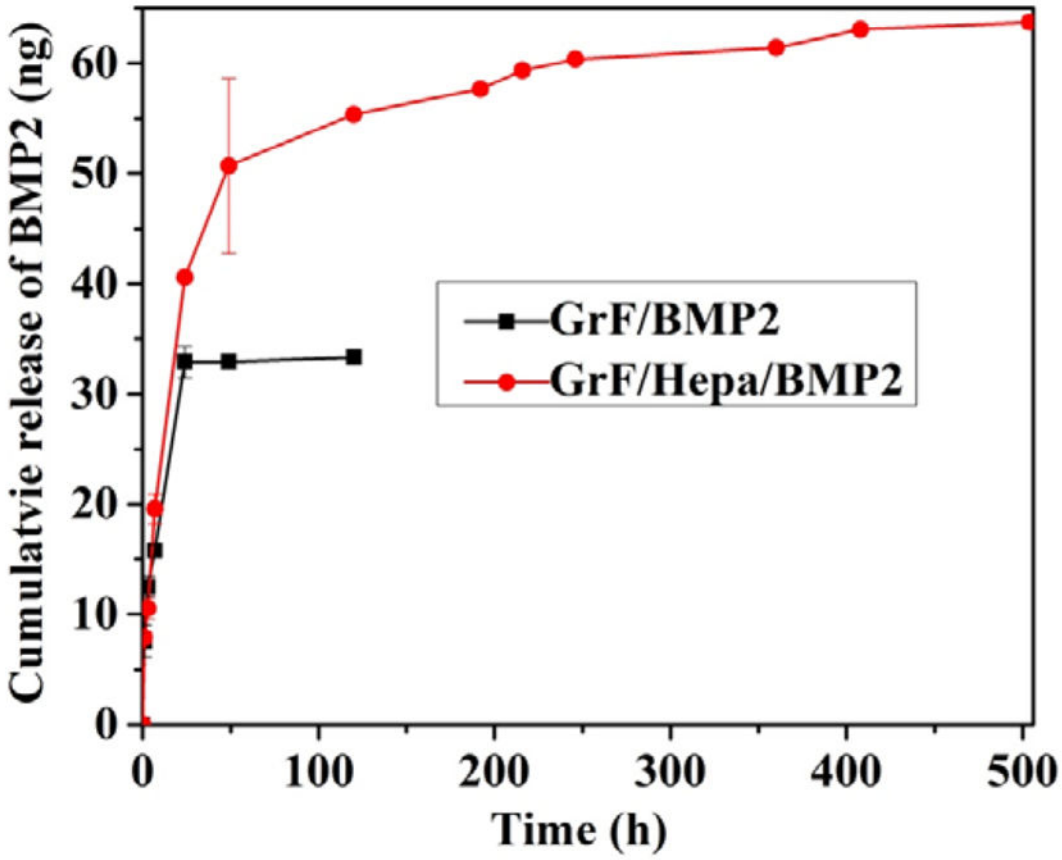

Figure 5.
In vitro BMP2 release behavior of samples in PBS at 37 ºC for a period time (n=3).

Author Manuscript Author Manuscript Author Manuscript Author Manuscript

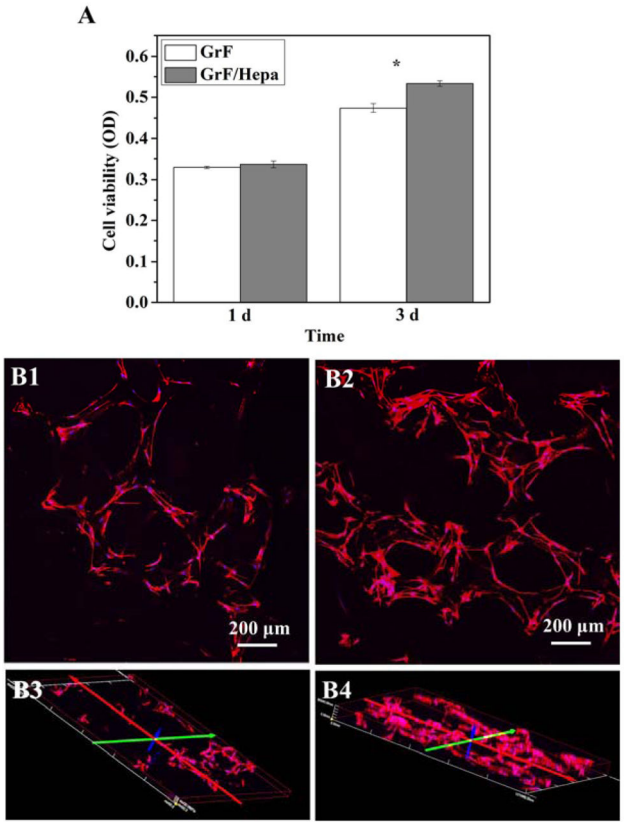

Figure 6.

(A) C2C12 viabilities on GrF and GrF/Hepa scaffolds after 1 and 3 days of culture. Cell morphologies on GrF (B1&3), GrF/Hepa/Dopa (B2&4) scaffolds after 3 days of culture. Scale bars=200 μm. Data are expressed as mean ± SD (n = 3). *p<0.05.

Author Manuscript Author Manuscript Author Manuscript Author Manuscript

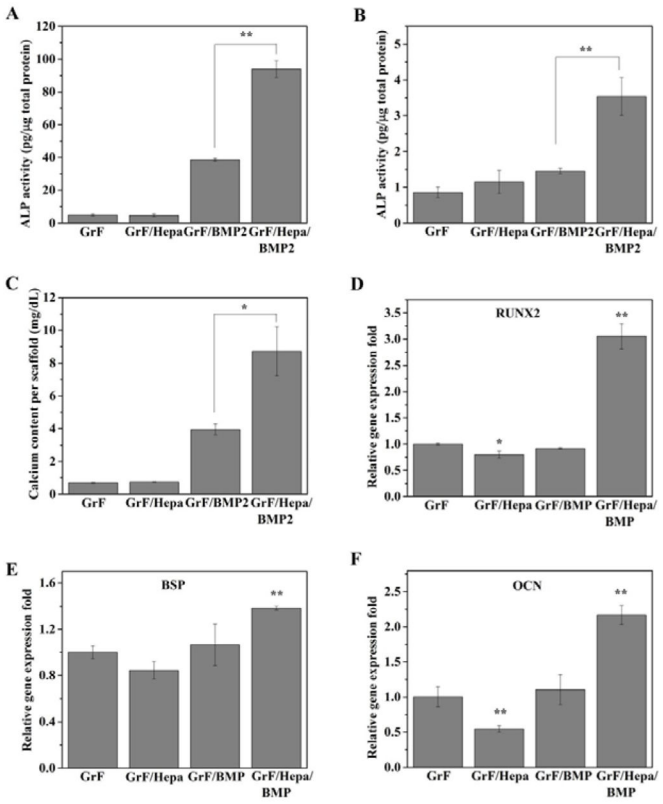

Figure 7.

ALP activity of C2C12 for 7 and 14 days (A, B) and total calcium content produced by hMSCs (C) cells cultured on GrF, GrF/Hepa, GrF/BMP2 and GrF/Hepa/BMP2 scaffolds. Osteogenic gene expressions (D. RUNX2, E. BSP, and F. OCN) were studied by real-time PCR assay after 7 days of culture on the scaffolds. Data are expressed as mean ± SD (n = 3). $*p < 0.05$, $**p < 0.01$.

Author Manuscript

Author Manuscript

Author Manuscript

Author Manuscript

Table 1

Surface elemental compositions of GrF, GrF/Hepa and GrF/Hepa/BMP2.

Substrate	C%	N%	O%	S%
GrF	85.79	0.05	11.01	0
GrF/Hepa	72.22	3.08	22.75	1.95
GrF/Hepa/BMP2	67.24	9.01	22.67	1.08

Author Manuscript

Author Manuscript

Author Manuscript

Author Manuscript

Table 2

The contact angle of GrF and surface modified GrF scaffolds.

Scaffold type	Contact angle (°)
GrF	107.4±3.8
GrF/BMP2	74.8±6.2
GrF/Hepa	67.2±5.9
GrF/Hepa/BMP2	32.5±3.9